Reprinted from the *British Journal of Applied Physics*, Vol. 14, pp. 904–907, December 1963

Applications of 'limited projection topographs' and 'direct beam topographs' in diffraction topography

A. R. LANG
H. H. Wills Physics Laboratory, University of Bristol
MS. received 2nd August 1963

The method of projection topographs can be modified so that images are recorded only from imperfections which lie within a chosen range of depths in the crystal specimen. This technique of 'limited projection topographs' allows easier study of internal imperfections by eliminating images of surface damage. It can also be applied in studying imperfections just below a crystal surface, as in correlating dislocation outcrops with surface features. Another modification uses multiply scattered radiation leaving the crystal in the direction of the direct beam to produce 'direct beam topographs' which have different contrast characteristics from the usual diffracted beam topographs.

1. Introduction

The method of x-ray 'projection topographs' (Lang 1959) was designed to present an easily interpretable overall picture of the distribution of lattice imperfections within a crystal. The image recorded on the topograph is a projection of the entire crystal volume scanned by the incident x-ray beam, the direction of projection being that of the diffracted rays of the chosen Bragg reflection. The area of specimen scanned during an exposure is limited only by the maximum available height of incident beam and by the maximum range of the linear traversing mechanism carrying the specimen. Specimen thickness is obviously limited by absorption of the x-rays, but with light elements and radiations such as MoKα, AgKα and WKα, specimens up to several millimetres thick can be used. However, with thicker specimens it may often happen that one wishes to concentrate study only on a certain range of depths within the crystal, and to do this without mechanically thinning the specimen. This need arises when the specimen surfaces are unrepresentative of the bulk specimen to an appreciable depth, or when the specimen has surface damage which it is impossible, or not desired, to remove. Also, since imperfections lying throughout the whole depth of crystal have their images superimposed on the projection topographs it follows that the capacity for resolving individual defects (such as dislocations) decreases as the specimen thickness is increased. If the specimen could be examined layer by layer in turn, less crowded patterns of dislocations would be obtained. These requirements may be met by use of the 'limited projection topograph' described in § 2, an arrangement which usefully enlarges the field of application of x-ray topographic methods.

In the usual experimental arrangement for taking projection topographs the beam incident upon the specimen is not collimated by reflection at a monochromator crystal; in fact, the use of an incident beam whose angular divergence is wider than the natural angular width of reflection of a perfect region of the specimen contributes to the production of high diffraction contrast at imperfections, when the specimen is lightly absorbing. Occasionally this high contrast is not required, and is indeed undesirable when it comes from locally intensely deformed regions such as those surrounding cracks, inclusions and surface scratches. In such cases a more strictly collimated incident beam is wanted in order to prevent highly misorientated regions from giving their intense Bragg reflections. Strict collimation may be achieved by use of the double or triple crystal spectrometer arrangements, but at the cost of considerable complication of the instrumentation and the necessary adjustments, and of great sensitivity to thermal and mechanical instability. One very simple way of achieving the effects of strict collimation is to use the specimen crystal itself as its own 'crystal collimator'. In this technique the topograph image is produced by radiation which has undergone multiple reflection in the specimen crystal and which leaves the crystal in the direction of the incident beam. Such a diffraction arrangement may be called 'direct beam projection topography' and will be more fully described in § 3.

2. Limited projection topographs

Figure 1 shows in plan several variants of the experimental arrangements for taking projection topographs. The incident beam, which has the form of a narrow ribbon perpendicular to the plane of the drawing, cuts the specimen crystal C along OA. Bragg reflection occurs at planes

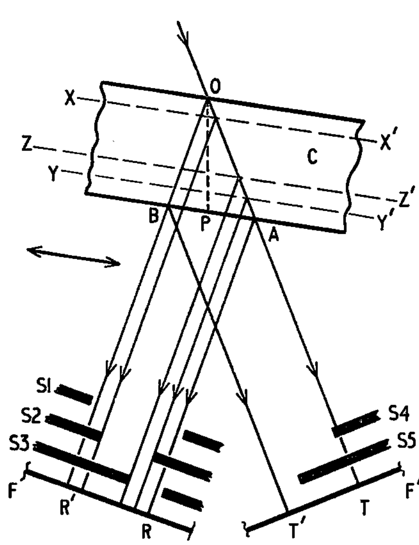

Figure 1. Aperture settings for 'limited projection topographs' and 'direct beam topographs'.

parallel to OP, giving rise to diffracted rays such as OB. The photographic emulsion is placed at F to record diffracted beam topographs or at F′ to record direct beam topographs. (If a thin emulsion is used, so that oblique incidence does not lead to significant loss of resolution, both the diffracted beam topograph and the direct beam topograph can be received on the same plate, set perpendicular to OP.) During the course of exposure the plate and the specimen are together translated backwards and forwards parallel to the double-headed arrow in order that the entire specimen volume of interest is cut by the direct beam OA. In the standard arrangement for taking projection topographs the aperture in the stationary screen between C and F is set like S1. For diffracted beam topographs this screen does, of course, extend sufficiently on either side of the diffracted beam to intercept the direct beam and any unwanted other x-ray reflections. Diffracted rays are received on F from the whole depth of the crystal: rays directly diffracted from the point O on the entrance surface travel along BR′ and those directly diffracted from the point A on the exit surface travel along AR. The aperture required in S1 is a minimum when the direction of specimen traverse is made parallel with the entrance and exit surfaces (if they are parallel to each other) or with the mean plane of the specimen (if it tapers). The specimen mean plane is usually set normal to the plane of the incident and diffracted beams.

Figure 2 is a diffracted beam projection topograph of a natural diamond octahedron. The crystal surfaces are much damaged by ring-cracks and scratches and the topograph is

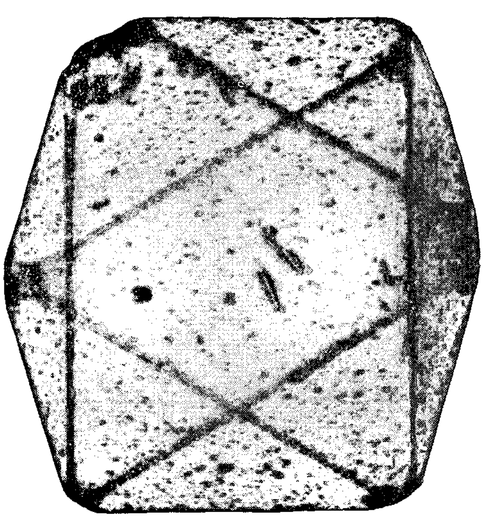

Figure 2. Projection topograph of diamond octahedron, edge length ~5 mm, 111 reflection, MoKα.

covered by their intense diffraction images. The strong diffracted intensity produced by the extra damage at edges and corners outlines the projection of the octahedron. Stereo-pairs of projection topographs show that the strong spot seen to the left of the topograph centre comes from an inclusion within the stone, but a cursory examination of the topographs suggests that there are no other internal imperfections. As is shown by its symmetry, the topograph of figure 2 was taken with a pair of octahedral faces set normal to the plane of the incident and diffracted beams. Hence these faces correspond to the x-ray entrance and exit surfaces of the specimen C drawn in figure 1. Now let the aperture in S1 be replaced by the reduced aperture S2. The only rays directly diffracted from the incident beam and admitted by S2 are those originating within the volume between the planes XX′ and YY′. Hence, over most of the topograph, no directly diffracted rays coming from the damaged faces of the crystal can reach F. On the resulting 'limited projection topograph', figure 3, almost the same effect is achieved as if the damaged entrance and exit surfaces had been

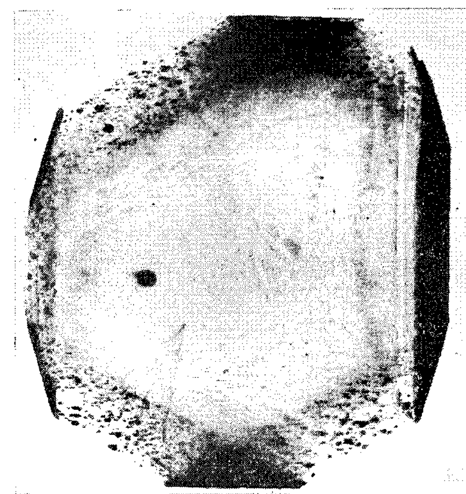

Figure 3. Limited projection topograph corresponding to complete projection topograph, figure 2.

physically removed. Defects within the interior of the crystal are more easily detected since the obscuring background of surface damage has been eliminated. In particular, about half a dozen dislocations, radiating from a small inclusion situated below the major inclusion, are now seen clearly. In the full projection topograph (figure 2) they are largely hidden by surface damage and can be recognized only by careful examination.

Another application of the limited projection topograph is shown in figures 4(a) and 4(b). The specimen is a plate of silicon, about 1·2 mm thick, cut roughly parallel to one of the slip-planes, which are of the type $\{111\}$. There is no surface damage problem here since the crystal can readily be etched. Dislocations lie in the slip-planes parallel to the specimen, at various levels within it, and also to some extent on the other $\{111\}$-type slip-planes steeply inclined to the specimen plate. Since the specimen is relatively thick, and images of dislocations in silicon formed with AgKα radiation are rather broad, the full projection topograph, figure 4(a), becomes confused at a relatively low dislocation density. Some clarification of the dislocation distribution can be gained by examining the specimen layer by layer. Figure 4(b) is a limited projection topograph of the same region as figure 4(a), taken with the same Bragg reflection but with the diffracted-beam aperture in the position S3 of figure 1. This setting allows directly diffracted rays to reach F from about one-third of the thickness of the crystal. Hence those dislocation loops lying within this fraction of the specimen thickness, from the exit surface down to the plane ZZ′, may be clearly identified.

The fraction of the full diffracted-beam width RR′ which is allowed to reach F may be made as small as desired, and in practice this selection is facilitated by a micrometer adjustment. However, the necessarily finite width of the direct beam OA (for which 12 to 15 μm is probably the practicable minimum value) imposes some uncertainty on the definition of location of the planes XX′, YY′ and ZZ′. One obvious application of the S3 arrangement, in which the exit surface and a small depth below it is selected for examination, lies in the correlation of dislocation outcrops with visible surface features on the crystal. An example of such work is the finding that pyramidal trigons on diamond octahedral faces coincide with dislocation outcrops (Lang 1964). The limited projection topograph technique may find useful application in studies of epitaxial growth on relatively thick substrates.

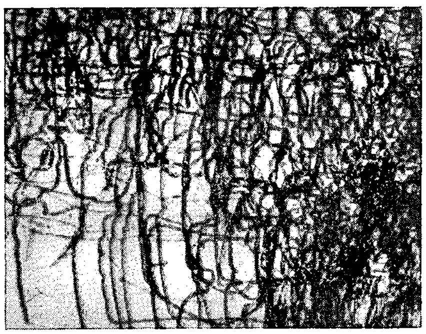

(a)

(b)

Figure 4. (a) Projection topograph of silicon plate, field width 3 mm, 220-type reflection, AgKα. (b) Limited projection topograph corresponding to figure 4(a), showing one-third of full specimen depth.

The greatest contribution to the high diffraction contrast manifested by imperfect regions (under conditions of relatively low x-ray absorption) comes from the 'direct diffraction image' formed when the imperfection is cut by the direct beam OA. As has been shown, any of these diffracted rays can be prevented from reaching the emulsion, as need arises. However, faint images of imperfections can still be produced by other mechanisms. For example, near the centre of the full projection topograph, figure 2, the direct images of two bad scratches are seen. In figure 3 these direct images are eliminated but the scratches are still faintly visible by their effect on other diffracted rays passing through them. Also, both experiment and theory show that rays participating in the process of multiple coherent scattering within a relatively perfect crystal fan out in all directions included between the primary beam and diffracted beam direction (see, for example, von Laue (1960)). Such rays, originating at or passing through an imperfection slight enough only to disturb but not destroy the multiple scattering process, produce a weak diffuse 'dynamical diffraction image' of the imperfection. When the imperfection is near O (figure 1) its dynamical image spreads over most of the base AB of the triangle OAB, and is hence difficult to eliminate by any setting of the diffracted-beam slit. The diffuseness of the dynamical image in this case makes it unimportant. It is possible, however, to use the technique of limited projection topographs to enhance the contrast of the dynamical images of slight imperfections in nearly perfect crystals. In the fan of rays included between the direct and diffracted beam directions it is the central ones, flowing parallel to the Bragg planes OP, which are the most sensitive to slight crystal distortions. Hence a slit-setting such as S2, which admits rays coming from P but intercepts those coming from the margins of the diffracted beam, increases sensitivity in the detection of very weak lattice distortions. It has been used successfully to enhance the contrast of projection topograph images of oxygen bands in crucible-grown silicon crystals.

3. Direct beam topographs

If the range of misorientations of the crystal is small then multiple scattering of x-rays will occur within the triangle AOB whenever the incident beam OA covers the angular range of Bragg reflection of planes parallel to OP. A natural result of such multiple scattering is that the direct beam is spread out laterally from AT to BT′. The expected intensity profiles across the diffracted beam RR′ and the direct beam TT′ can be calculated from the dynamical theory of x-ray diffraction when the crystal is sufficiently perfect for the multiple scattering to occur coherently (Kato 1960). The intensity across TT′ falls off rapidly from T to T′ in cases of low or moderate x-ray absorption, i.e. when the product of linear absorption coefficient and crystal thickness does not exceed a value of about 4. However, if a screen is placed to cut into the edge of the direct beam, as S4, figure 1, just far enough to intercept radiation in the incident beam which has not undergone Bragg reflection, but not enough to intercept an appreciable fraction of the multiply scattered rays reaching TT′, then projection topographs can be obtained with the remainder of the direct beam comparable in intensity with the usual diffracted beam topographs. In simple terms, the essential difference between the 'direct beam topographs' thus obtained and diffracted beam topographs is that the images in the former are produced by rays which have undergone at least two reflections in the crystal. Some of the conditions of the double-crystal spectrometer arrangement are thereby simulated. It follows that in direct beam topographs there is a great reduction in the intensity of the direct images of imperfections, for all parts of the specimen. The sensitivity to small lattice distortions is not reduced, for perturbations of the sensitive rays, which flow parallel to OP, affect the direct and diffracted beams equally, but in opposite sense.

Figure 5(a) is a diffracted beam projection topograph of a natural diamond octahedron. The usual damage to faces and edges is evident. In addition, dislocations radiating from the centre of the stone may be seen. The direct beam projection topograph, taken at the same time, appears rather different in shape due to the difference in projection directions, the angle between direct beam and diffracted beam being 33° for MoKα radiation and the 220 reflection. On figure

5(*b*) the strong images from misoriented regions surrounding surface damage are greatly reduced in intensity, for all surfaces. The dislocations can still be seen fairly clearly.

Various mechanisms contribute to the diffraction contrast of dislocations on x-ray topographs. A comparison of diffracted beam and direct beam topographs throws some light on their working. In cases of low x-ray absorption and

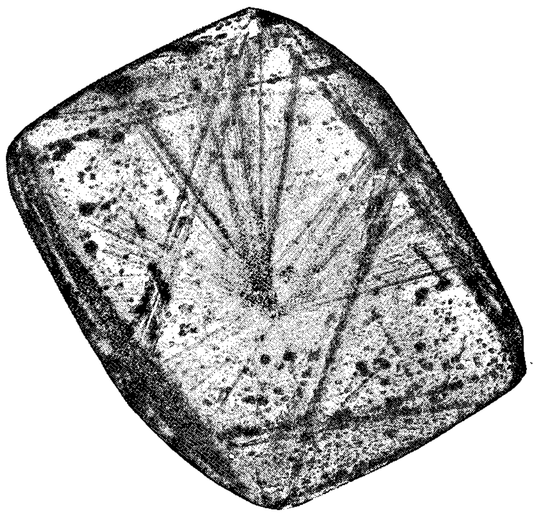

(*a*)

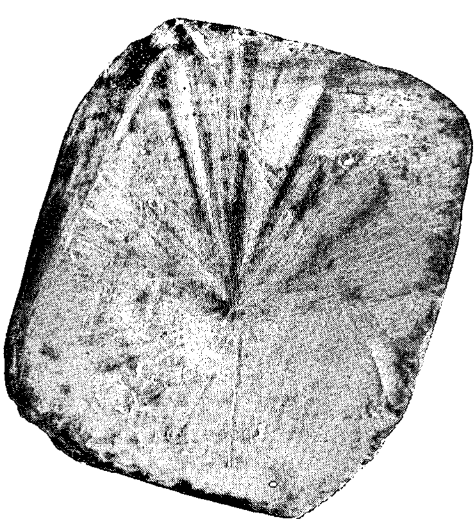

(*b*)

Figure 5. (*a*) Diffracted beam projection topograph of diamond octahedron, edge length ~5 mm, 220-type reflection, MoKα. Note that the apparent doubling of the image of the left-hand octahedral face is not an experimental artefact but a genuine diffraction effect due to an imperfect layer 200 μm below this face.

(*b*) Direct beam topograph corresponding to figure 5(*a*).

low x-ray scattering factor the very strong direct image of dislocations comes from regions surrounding the dislocation which are very slightly misoriented from the perfect matrix yet which effectively diffract independently of it as far as phase relationships are concerned. These misoriented regions, some micrometres in diameter, behave similarly to an imperfect crystal and have a strong reflecting power. As already mentioned, in a perfect crystal a fan of coherently scattered x-rays fills the whole of the triangle OAB. Thus, in the triangle, near A the energy flow is nearly parallel to OA, and near B it is nearly parallel to OB. Also, in the case of low x-ray absorption, the energy flow at A is much stronger than at B. It is to be expected, then, that a dislocation near the exit surface, acting as a strong x-ray reflector, will divert the dominant energy flow from the AT to the AR directions when situated near A, and from the BR′ to BT′ directions when near B. This phenomenon has been well observed with silicon crystals and AgKα radiation. It is illustrated by the following experiment. With the screen setting S4, the direct beam topograph is formed predominantly by rays travelling close to AT on account of the above-mentioned distribution of energy flow across AB and the resulting fall-off in intensity, from T to T′, of rays reaching F′. Thus the type of contrast on the direct beam topograph given by dislocations near the exit surface will be governed by their effects when near A. Since at this point they divert energy away from the direct beam direction they will appear as light lines on a darker background, i.e. with contrast opposite to that exhibited on diffracted beam topographs. Figure 6(*a*) is a diffracted beam topograph of an array of dislocations close to the exit surface in a plate of silicon. Figure 6(*b*) is the direct beam topograph of the same region of the crystal, with the screen set as S4. If the screen is pushed far into the direct beam, into the position S5, then, as expected, contrast of the same type as in figure 6(*a*) is regained, but the overall intensity of the pattern is weak.

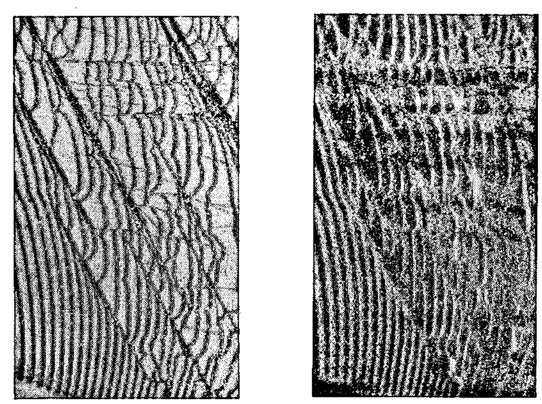

(*a*) (*b*)

Figure 6. (*a*) Projection topograph of silicon plate, field width 1·7 mm, 220-type reflection, AgKα. (*b*) Direct beam topograph of field of figure 6(*a*), 440-type reflection, AgKα.

Acknowledgments

The author gratefully acknowledges financial support from the Metallurgy Branch, United States Office of Naval Research, for that part of the work done at Harvard University, and from the Aeronautical Research Laboratory, Office of Aerospace Research, for support subsequently, through the European Office, Aerospace Research, United States Air Force.

References

Kato, N., 1960, *Acta Cryst.*, **13**, 349.

Lang, A. R., 1959, *Acta Cryst.*, **12**, 249.

——1964, *Proc. Roy. Soc. A.*, in the press.

von Laue, M., 1960, *Röntgenstrahlinterferenzen* (Frankfurt a. M.: Akad. Verlag).

UNWIN BROTHERS LIMITED, WOKING AND LONDON